



SCHOOL of
GRADUATE STUDIES
EAST TENNESSEE STATE UNIVERSITY

East Tennessee State University
**Digital Commons @ East
Tennessee State University**

Electronic Theses and Dissertations

Student Works

5-2016

Immobilization of Heteropolyacids in Silica Gel

Opeyemi Adetola

East Tennessee State University

Follow this and additional works at: <https://dc.etsu.edu/etd>

 Part of the [Analytical Chemistry Commons](#), [Environmental Chemistry Commons](#), and the [Materials Chemistry Commons](#)

Recommended Citation

Adetola, Opeyemi, "Immobilization of Heteropolyacids in Silica Gel" (2016). *Electronic Theses and Dissertations*. Paper 3050.
<https://dc.etsu.edu/etd/3050>

This Thesis - Open Access is brought to you for free and open access by the Student Works at Digital Commons @ East Tennessee State University. It has been accepted for inclusion in Electronic Theses and Dissertations by an authorized administrator of Digital Commons @ East Tennessee State University. For more information, please contact digilib@etsu.edu.

Immobilization of Heteropolyacids in Silica Gel

A thesis
presented to
the faculty of the Department of Chemistry
East Tennessee State University

In partial fulfillment
of the requirements for the degree
Master of Science in Chemistry

by

Opeyemi Adetola

May 2016

Dr. Aleksey N. Vasiliev, PhD, Chair,

Dr. Gregory W. Bishop, PhD

Dr. Dane W. Scott, PhD

Keywords: Heteropoly acids, Phosphomolybdic acid, Phosphotungstic acid, Sol-gel, Mesoporous materials, Surfactants, X-ray diffraction, Small angle X-ray scattering.

ABSTRACT

Immobilization of Heteropolyacids in Silica Gel

by

Adetola Opeyemi

Silica gels containing incorporated heteropolyacids (HPAs) were synthesized in acidic media by co-condensation of tetraethoxysilane (TEOS) with phosphotungstic or phosphomolybdic acids using sol-gel technique. Effect of the synthesis conditions on their structure and morphology was studied. Yields of modified materials were some lower as compared to non-modified silica gels. All materials were mesoporous but contained micropores in their structures. Presence of bands of Keggin's structures in FT-IR spectra along with absence of XRD patterns of crystalline HPAs confirmed their fine incorporation into silica network. Particle sizes of modified materials were 800-1100 nm excepting for W-containing sample obtained with trimethylstearylammmonium chloride. This unusual effect was attributed to stabilization of primary silica nanoparticles by interaction between surfactant and HPA. High ratio HPA/TEOS resulted in partial loss of porosity. Obtained results might be used for optimization of synthesis of effective catalysts and adsorbents containing HPAs in mesoporous structure.

DEDICATION

This work is dedicated to my parents: my father, Mr. Adetola Adebajo Ezekiel and my mother Mrs. Adetola Oluwabunmi Christianah. My brother: Adetola Abimbola, My sisters: Mrs. Oyebajo Oyindamola and Adebajo Mercy. My Mentor: Mr. Oluseye Oshunpidan and Audam Timothy.

ACKNOWLEDGEMENTS

This work was supported by NATO's Emerging Security Challenges Division in the framework of the Science for Peace and Security Programme (grant SfP 984639) and by School of Graduate Studies, East Tennessee State University (grant E85033).

We thank Dmytro Molodyi and Sergyi Bohvan for their assistance in XRD and SAXS study and TEM imaging of the materials. We also thank Dr. Reza Mohseni for the AAS analysis of materials.

I would start by saying a heart-felt thank you to Dr. Aleksey Vasiliev for his mentorship and support during my research.

I express my sincere appreciation to Dr. Dane Scott and Dr. Gregory Bishop for serving as committee members for my thesis. I want to also use this medium to thank the following people: Acquah Chris, Freddy Sime, Emmanuel Onobun, and Joseph Osazee for their support during the course of this work.

TABLE OF CONTENTS

	Page
ABSTRACT	2
DEDICATION	3
ACKNOWLEDGEMENTS	4
LIST OF TABLES	8
LIST OF FIGURES	9
Chapter	
1. INTRODUCTION.....	10
Mesoporous Materials.....	10
Sol-Gel Process	12
Heteropolyacids	15
Modification of Porous Materials by HPAs.....	17
Impregnation	17
Co-Condensation.....	18
Research Objective	19
2. EXPERIMENTAL.....	20
Chemicals	20
Precursors	20
Surfactants.....	20
Reagents	20
Synthetic Procedures	22
Standard Condition of synthesis	22

	Study of Effect of Hydrochloric acid.....	23
	Study of Effect of Concentration of Surfactant	23
	Study of Effect of Reaction Time and Aging	23
	Study of the Effect of Precursors	23
	Chemical Composition.....	24
	Atomic Absorption Spectroscopy (AAS)	24
	Fourier Transform Infrared Spectroscopy (FT-IR).....	24
	Structure of Materials	24
	Porosimetry.....	24
	Particle Size	24
	X-ray Diffraction (XRD)	25
	Small Angle X-ray Scattering (SAXS).....	25
	Transmission Electron Microscope (TEM)	25
3.	RESULTS AND DISCUSSION.....	26
	Chemical Composition.....	26
	Samples Synthesized In Standard Conditions.....	26
	Effects of Varying Conditions	27
	Fourier Transform Infrared Spectroscopy	29
	Structural Characteristics	30
	Porosity of Samples	30
	Particle Size and Polydispersity Index (PDI).....	33
	X-RAY Diffraction and Small Angle X-ray Scattering.....	33
	TEM Imaging.....	35

Discussion.....	36
Conclusions.....	39
REFERENCES	40
VITA.....	45

LIST OF TABLES

Table	Page
1. Different Precursors Used.....	20
2. Different types of surfactants Used.....	21
3. Synthesis of samples in standard conditions.....	26
4. Yields and HPA contents of samples prepared at different conditions	27
5. Porosity of samples	31
6. Particle size and PDI.....	34

LIST OF FIGURES

Figure	Page
1. Different structures of the M41S family: (top) surfactant supramolecular assemblies and (bottom) TEM images of the final materials.....	11
2. Mesoporous quasicrystals	12
3. Reactions of Sol-Gel synthesis	13
4. Formation of Porous Structure at the Use of Surfactants in Sol-Gel Synthesis.....	13
5. Cationic Surfactant: benzalkonium chloride.....	14
6. Anionic Surfactant: sodium stearate	15
7. Non-ionic Surfactant: lauryl glucoside	15
8. Amphoteric Surfactant: phosphatidylcholine	15
9. Steps in Catalyst Synthesis via Impregnation.....	17
10. Schematic illustrating the nucleated-growth synthesis of OMC-supported noble metal and intermetallic nanocrystallites using impregnation method	18
11. Flowchart of synthesis of mesoporous materials	22
12. FT-IR spectra of the materials	29
13. Nitrogen adsorption isotherms on materials obtained with different templates	30
14. XRD (a) and SAXS (b) curves of the materials, obtained with P-123	35
15. TEM images of non-modified, Mo-containing and W-containing silica gel.....	35
16. Particle size distribution in samples obtained with TMS.....	37

CHAPTER 1

INTRODUCTION

Mesoporous Materials

An in-depth understanding of materials with respect to their porosity is very important because of their popular use in recent applications like drug delivery and catalysis. Mesoporous materials are materials that have pore sizes between 2-50 nm in diameter and microporous and macro porous less than 2 nm and greater than 50 nm respectively.

Mesoporous materials have been applied in many liquid phase catalytic processes [1] and the uniformity of their pore channels with high surface area and larger pore diameter is widely used for the development of novel solid catalysts [2]. Researchers have proved that mesoporous materials can overcome the pore size constraint of microporous zeolites and allow more facile diffusion of bulk substrates [3]. After incorporation of large catalysts, an unrestricted diffusion of both reactants and products were observed for materials that are mesoporous [4, 5].

Recently, increasing research interest focuses on the replacement of hazardous Lewis and Brønsted acid catalysts for heterogeneous analogues, particularly for reactions involving molecules that are too large to access the small cavities of acid zeolites. Solid acid catalysts, which are recyclable and readily separable from the reaction system, offer the opportunity to reduce the impact on the environment and increase industrial interest for the liquid phase acid catalytic process [1, 6]. For this purpose, heterogenization of active species onto the suitable mesoporous inorganic or inorganic-organic hybrid frameworks is one of the efficient ways to develop the novel solid acid catalysts, which can result in an improvement of the overall efficiency of the process [7].

Many preparation methods of mesoporous silica materials with various morphologies from thin film, sphere, fiber, as well as bulk form (Fig. 1), such as the MCM series [8] and the SBA series [9], have been reported. In these synthetic reactions, the organic template-driven synthesis process is commonly used.

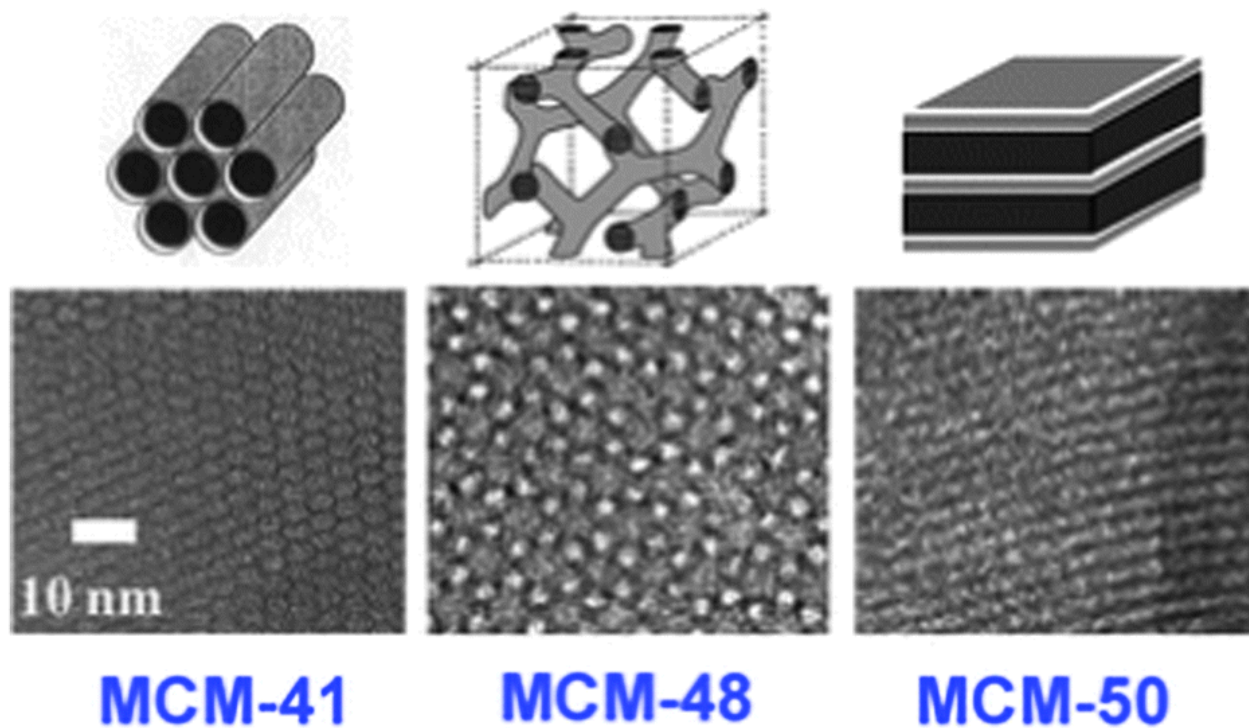


Figure 1: Different structures of the M41S family: (top) surfactant supramolecular assemblies and (bottom) TEM images of the final materials [10]

Mesoporous silica can also be synthesized by using templates of micellar rods reacting with TEOS which results in collection of nano-sized rods that have regular arrangement of pores [11]. Xiao et al. reported the synthesis of mesoporous quasicrystals (Fig. 2).

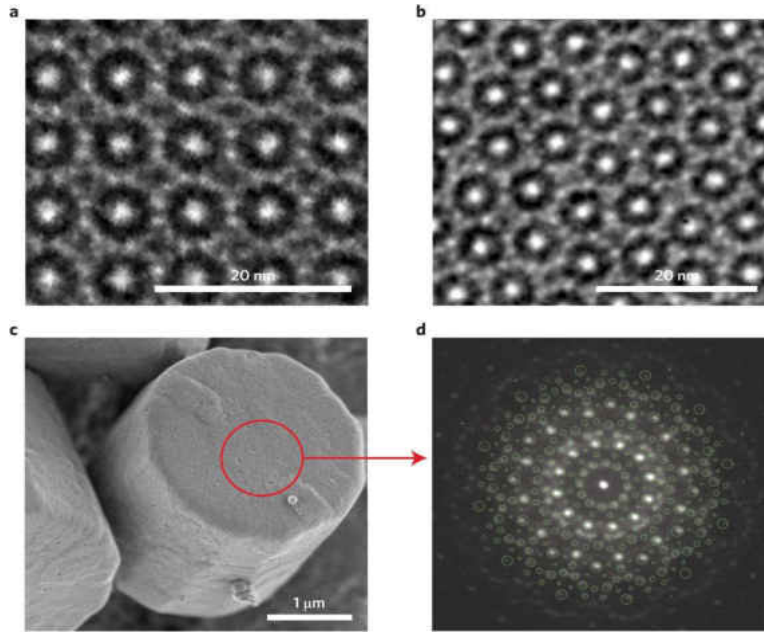


Figure 2: Mesoporous quasicrystals “the quasicrystals can be produced using synthetic conditions between those required to produce cubic (a) and tetragonal (b) mesoporous materials. (c) The resultant materials showing micrometer-scale grains with the morphology of a dodecagonal prism. (d) An electron diffraction pattern showing that the center of these grains show well-ordered quasicrystalline behavior” [12].

Sol-Gel Process

Sol-gel process is a technique that has been used widely in aspects of materials and ceramic science. It is used in the preparation of pure ceramic starting materials and inorganic glasses. The reaction is typically carried out in two steps: hydrolysis of metal alkoxides to generate hydroxyl groups, followed by polycondensation of the hydroxyl groups, and remaining alkoxy groups to form a three-dimensional structure. Common precursors that are used in this process includes metal alkoxides and metal chlorides [13].

The metal alkoxides belong to the family of metalorganic compounds with an organic ligand attached to a metal atom. The common type of metal alkoxides used is silicon tetraethoxide

which is commonly called tetraethylorthosilicate (TEOS) with chemical formula $\text{Si}(\text{OC}_2\text{H}_5)_4$. In this process the sol forms a gel-like network which contains 2 different phases; solid and liquid. The hydrolysis and condensation reactions occur simultaneously once the hydrolysis reaction has been initiated (Fig.3).

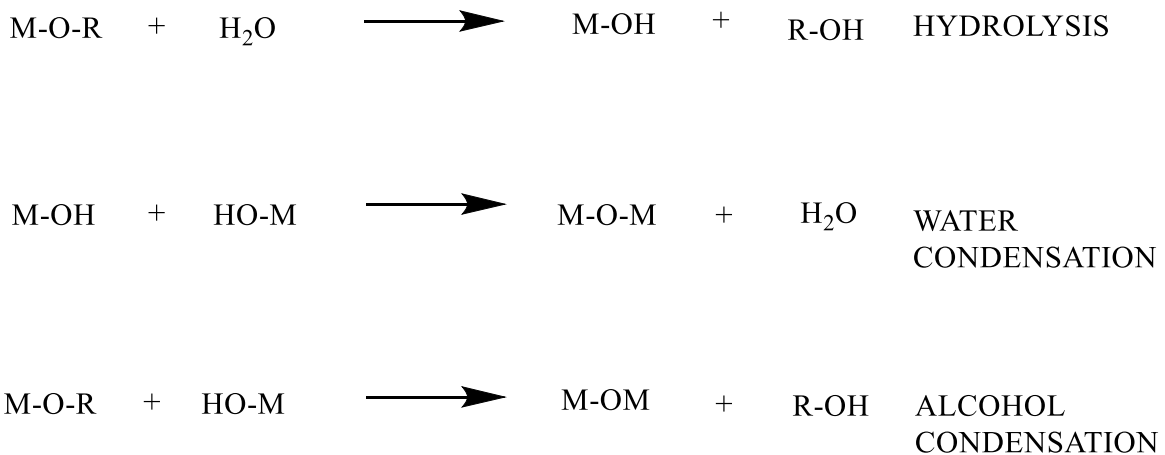


Figure 3: Reactions of sol-gel process

Ordered mesoporous materials are made with a combination of using self-assembled surfactants as template and simultaneous sol-gel condensation around template (Fig. 4).

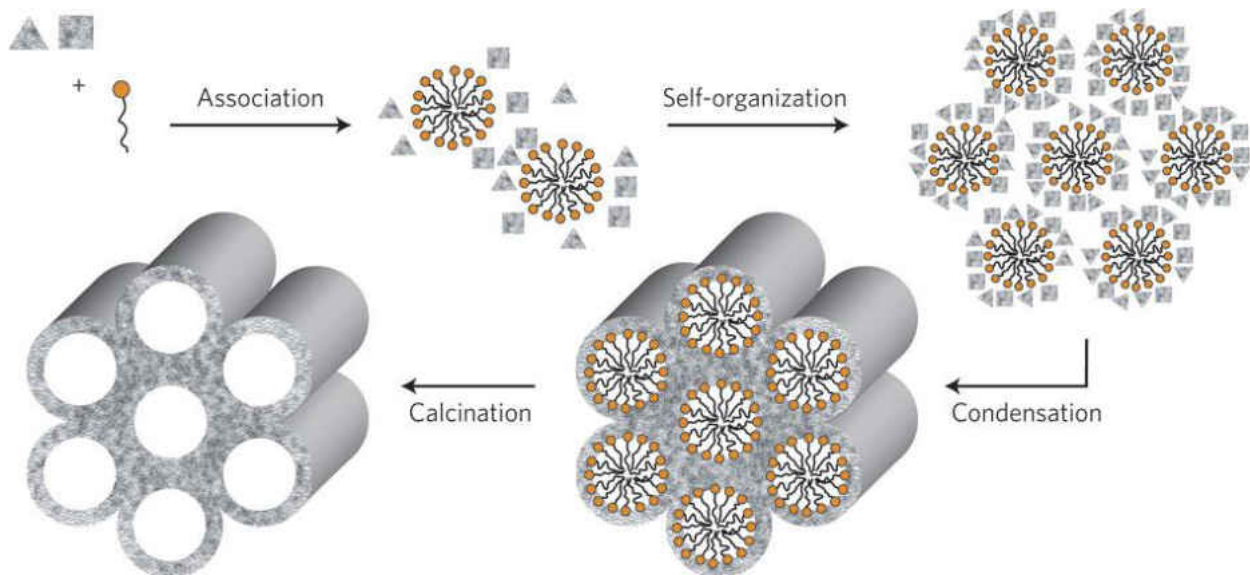


Figure 4: Formation of porous structure at the use of surfactants in sol-gel synthesis [12]

Micelles have been used as templates to synthesize mesoporous materials that are ordered by sol-gel synthesis [14].

Surfactants are organic molecules that are amphiphilic in polarity [15]. The hydrocarbon chain is nonpolar giving it its hydrophobic and lipophilic property, while the head is polar and hydrophilic. Surfactants diffuse in water and adsorb at the surface of a solution or interface between aqueous and hydrocarbon solvents, so that the hydrophilic head can turn towards the aqueous solution, causing a reduction in interface energy. Such concentration segregation is spontaneous and thermodynamically favorable. Due to the nature of their ordered arrangement of molecules in solution, the surface energy decreases as the concentration increases leading to the formation of micelles that changes shape from a spherical shape to a hexagonal pack of cylindrical micelles [16]. Surfactant molecules can be generally classified into 4 groups namely:

- a) Cationic surfactants: Cationic surfactants comprises of primary and secondary amines that are dependent on pH and quaternary ammonium salts. Examples include benzalkonium chloride (BAC) (Fig. 5), dodecylamine (DDA), and cetyltrimethylammonium bromide (CTAB) [16].

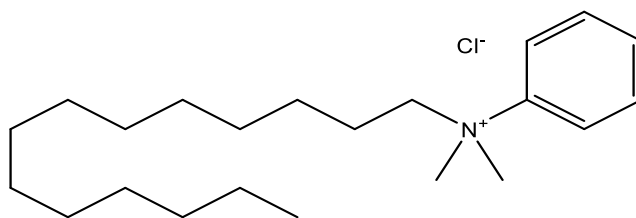


Figure 5: Cationic surfactant: benzalkonium chloride (BAC)

- b) Anionic Surfactants: Typical anionic surfactants include the sulfates, sulfonates, phosphate esters and carboxylates with an alkyl chain consisting of 11 to 21 carbon chains. Examples include sodium dodecyl sulfate (SDS) and sodium stearate (Fig. 6).

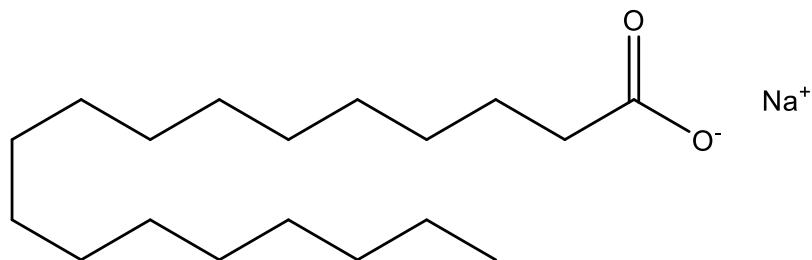


Figure 6: Anionic surfactant: sodium stearate

- c) Non-ionic surfactants: This group of surfactants do not dissociate into ions when dissolved in a solvent unlike the anionic and cationic surfactant. Their hydrophilic head is a polar group such as ether, RO-R, alcohol and R-OH, carbonyl, R-CO-R (Fig. 7).

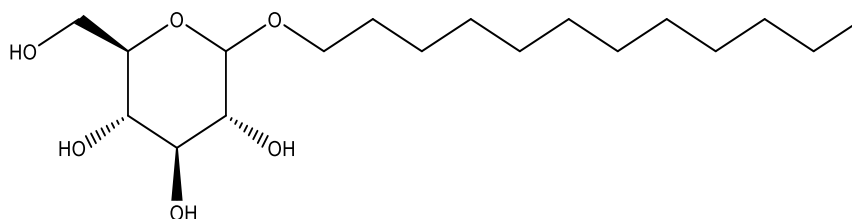


Figure 7: Non-ionic surfactant: lauryl glucoside

- d) Amphoteric / Zwitterionic surfactants: Amphoteric surfactants have both properties of nonionic surfactants or ionic surfactants (Fig. 8). Examples are betaines and phospholipids.

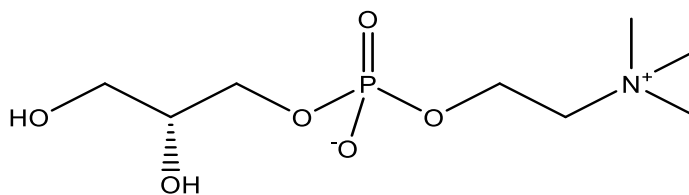


Figure 8: Amphoteric: phosphatidylcholine

Heteropolyacids (HPAs)

Heteropolyacids have polyoxometalate inorganic cage structures, which may adopt the Keggin form with the general formula $H_3MX_{12}O_{40}$, where M is the central atom and X the heteroatom. Typically M can be either P or Si, and X = W or Mo [17].

HPAs containing molybdenum or tungsten in their structures are highly active in various catalytic reactions, such as hydration, polymerization or condensation [18]. Their unique catalytic activity is the result of super acidity: they are much stronger Brønsted acids than HClO_4 or H_2SO_4 , and even stronger than high-silica zeolites, e.g. H-ZSM-5 [19, 20]. The strong acidity is caused by delocalization of negative charge on large anions with Kegging's structure [21]. The formation of super acids depends on hydrogen concentrations, concentration of phosphoric acid, concentration of W or Mo and temperature.

HPAs are used in petrochemical industry, in particular, for hydration of alkenes. However, their industrial use is limited by two essential disadvantages: low surface area ($\sim 5 \text{ m}^2/\text{g}$) and solubility in polar solvents. Materials with improved structural characteristics were obtained by impregnation of silica gel by a solution of $\text{H}_3\text{PW}_{12}\text{O}_{40}$ [17]. Their pore volumes and BET surface areas were sufficiently high but gradually decreased with increase of HPA contents. Obtained catalysts were successfully used in isomerization of α -pinene in non-polar solvent while the use of polar solvents resulted in complete leaching of HPA from the support [22].

An interesting property of HPAs is their ability to form insoluble salts with cations of alkali metals, which typically form well soluble salts with most of inorganic anions [23]. In particular, cesium salt $\text{Cs}_{2.5}\text{H}_{0.5}\text{PW}_{12}\text{O}_{40}$ has higher acidity and, as a result, superior catalytic activity in acid-catalyzed reactions [24]. This salt forms very fine colloidal particles that complicate their use in catalytic reactor due to small size [25, 26].

HPAs are strong Brønsted acids but they are highly soluble in polar solvents and will be very difficult to separate them from products. It is necessary to have a support in which they can be structurally incorporated with uniform shapes, sizes and specific surface area. Immobilization of HPAs on a functionalized support gives more stability and enhanced catalytic activity [27].

Modification of Porous Materials by HPAs

Impregnation

Impregnation is a common method for synthesis of heterogeneous catalysts. Impregnation process involves making a solid come in contact with a liquid containing the components to be deposited on the surface (Fig. 9).

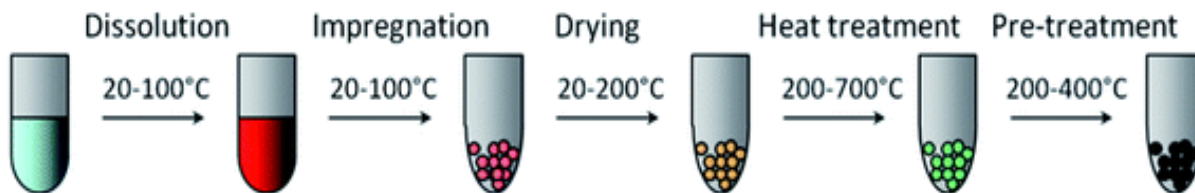


Figure 9: Typical steps in catalyst synthesis *via* impregnation [28].

There are different methods of impregnation which are explained below:

- Soaking or wet impregnation:** In this method the amount of liquid used is controlled by the solubility of support used with excess liquid been removed by evaporation. Deposition consumes time and loss of surface area may occur in the process.
- Incipient wet impregnation:** Volume of sample used must correspond to the pore volume of support and can only be used for species with weak surface interactions. Redistribution inside pores takes hours.
- Percolation Impregnation:** Ion exchange occurs by permeation of the impregnating solution through a carrier.
- Co-impregnation / successive impregnation:** In the former more than 1 active ingredients are introduced into a single step while in the later they are introduced step by step. The problem with this method is the inability to achieve a uniform distribution of species [29].

Ji et al [30] reported the chemically controlled process for synthesis of size-controlled noble metal embedded within the porous structure of ordered mesoporous carbon by impregnation (Fig.10).

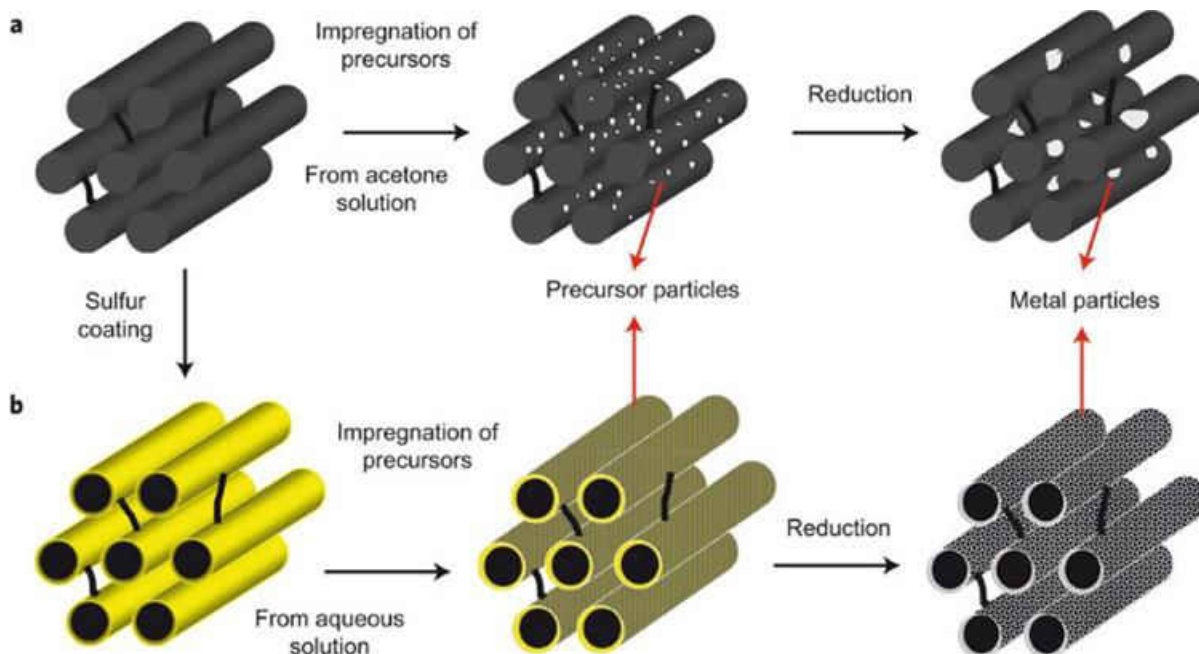


Figure 10: Schematic illustrating the nucleated-growth synthesis of OMC-supported noble metal and intermetallic nanocrystallites using impregnation method [30]

Co-Condensation

Co-condensation can also be called the one step reaction because it allows the synthesis and functionalization of silica with uniform distribution of organic groups both on and inside the pore. This is achieved by mixing a surfactant with a silica source which activates hydrolysis and condensation reactions to form a more structured network with uniform pores [31].

More prospective strategy for preparation of highly porous stable materials with high contents of accessible acidic sites is co-condensation of HPA with tetraethoxysilane (TEOS) by sol-gel synthesis [32, 33].



HPAs demonstrated high activity in condensation of phenol with levulinic acid. Other publications report similar catalytic materials in oxidation of benzaldehyde to benzoic acid [34], alkylation of o-xylene by styrene [35] and esterification of lauric acid by glycerol [36]. Kaleta et al reported that immobilization of HPA inside the channels of Si-MCM-41 mesoporous molecular sieve by means of chemical bonding with amine groups introduced into the system during a previous aminosilylation procedure resulted in the strong anchoring of heteropoly anions and prevented the HPA from leaching [37].

Kala Raj et al. also reported that anchoring of HPA on mesoporous material like SBA-15 and MCM-41 has proven to be effective in leaching problems [38]. Izumi et al. have prepared silica-supported Keggin-type HPAs by encapsulating HPAs into a silica matrix by a sol-gel technique by hydrolysis of TEOS to form a solid that can be separated easily [39]. Nowin'ska et al. reported the incorporation of heteropoly compounds of tungsten and molybdenum into SBA-3 via one-pot process [40]. Mingyuan et al. reported a successful method of immobilizing phosphomolybdic acids on polyaniline functionalized carbon supports. Their results indicated that the phosphomolybdic acid retained its Keggin structure and that it helps to reduce the average particle size of palladium nanoparticles [41].

Research Objective

In this work we report the synthesis of highly porous HPA-containing silica gels obtained by sol-gel method. The objective of this work was to study effects of the synthesis conditions on the characteristics of the materials. Obtained results might be used for optimization of synthesis of effective catalysts and adsorbents containing HPAs in mesoporous structure.

CHAPTER 2

EXPERIMENTAL

Chemicals

Precursors

Tetraethoxysilane, phosphotungstic acid hydrate (PTA), and phosphomolybdic acid (PMA) were used as precursors in the synthesis (Table 1).

Table 1: Different precursors used.

Precursors	Formula (M.W)	Supplier
Tetraethylorthosilicate (TEOS)	$\text{Si}(\text{OC}_2\text{H}_5)_4$ (208.3 g/mol)	Acros Organics, Morris Plains, New Jersey
Phosphotungstic acid hydrate (PTA)	$\text{H}_3\text{PW}_{12}\text{O}_{40} \cdot x\text{H}_2\text{O}$ (2880.05 g/mol)	Acros Organics, Morris Plains, New Jersey
Phosphomolybdic acid (PMA)	$\text{H}_3\text{PMo}_{12}\text{O}_{40}$ (1825.25 g/mol)	Acros Organics, Morris Plains, New Jersey

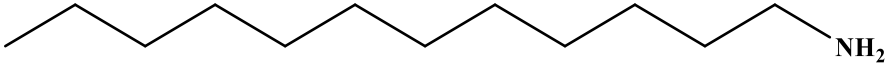
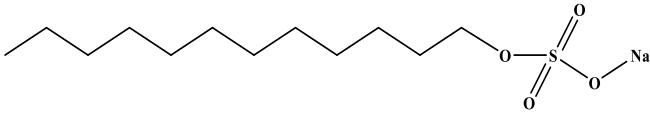
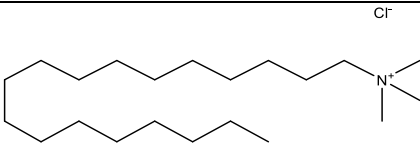
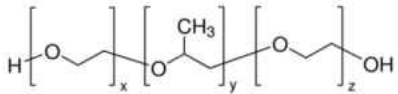
Surfactants

The following surfactants were used as templates: dodecylamine (DDA), sodium dodecylsulfate (SDS), trimethylstearylammmonium chloride (TMS) and Pluronic P-123 (Table 2)

Reagents

Hydrochloric acid, ethanol, acetone, hydrofluoric acid, sodium hydroxide, distilled water. All reagents were used as purchased without further purification.

Table 2: Different types of surfactants used

Surfactants	Type	Formula (M.W)	Supplier
Dodecylamine (DDA)	Cationic	$C_{12}H_{27}N$ (185.35 g/mol)	Acros Organics, Morris Plains, NJ
			
Sodium dodecyl sul- fate (SDS)	Anionic	$C_{12}H_{25}SO_4Na$ (288.37 g/mol)	Acros Organics, Morris Plains, NJ
			
Trimethylstearyl-am- monium chloride (TMS)	Cationic	$C_{21}H_{46}ClN$ (348.05 g/mol)	TCI, Tokyo, Japan
			
Pluronic (P-123)	Non-ionic	$HO(CH_2CH_2O)_{20}-$ $(CH_2CH(CH_3)O)_{70}-$ $(CH_2CH_2O)_{20}H$ (5800Da)	Sigma-Aldrich, St. Louis, MO
			

Synthetic Procedures

Standard Condition of Synthesis

Each of the surfactants were dissolved in 6 ml of ethanol. Separately, TEOS was dissolved in 2 ml of ethanol-heteropoly acid HPA solution and 3 ml of hydrochloric acid in 3 ml of water. Solutions of TEOS and aqueous acids were added dropwise to the solution of surfactant simultaneously at stirring. The reaction mixture was refluxed for 24 h. Obtained gel was filtered, washed by deionized water until complete removal of acid, then by acetone, and dried on air overnight (samples **1-12**). All samples were calcined at 500 °C for 5 h in a muffle furnace (Ramp rate: 25 °C – 537 °C, non-condensing, 85% max humidity). Yields were calculated in g per 1 g of TEOS + HPA (g_0).

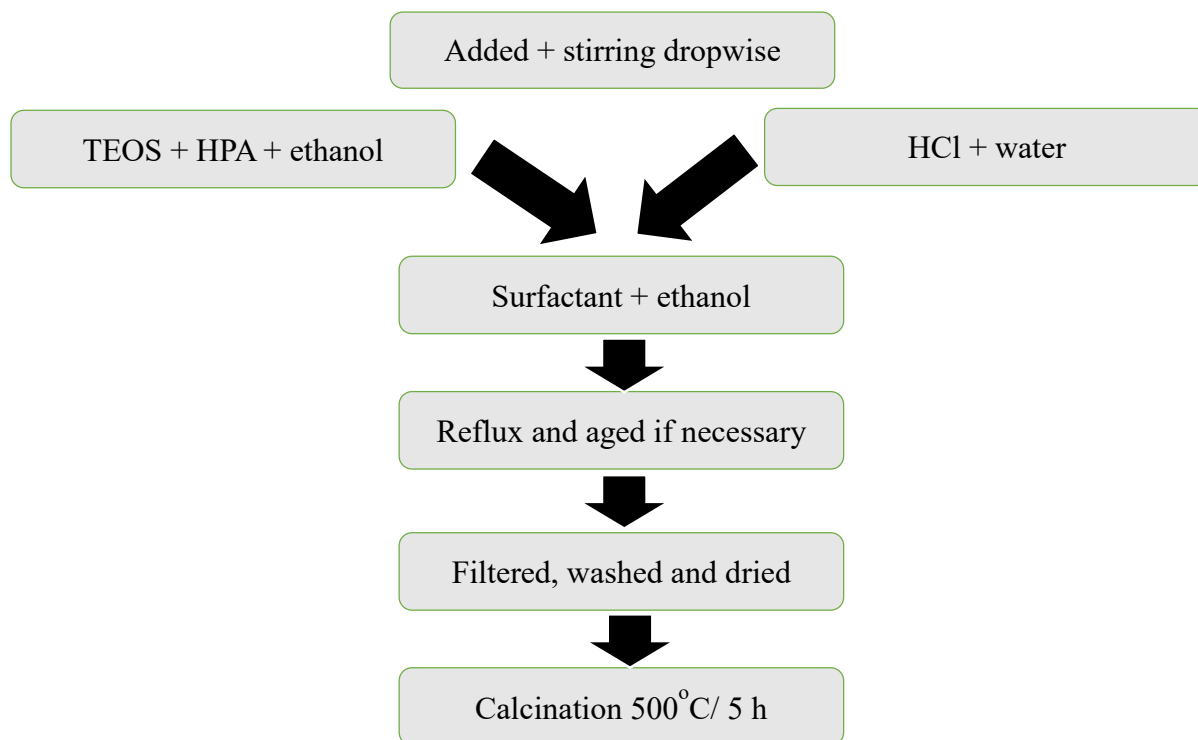


Figure 11: Flowchart of synthesis of mesoporous materials

Study of Effect of Concentration of Hydrochloric Acid

To study the concentration of hydrochloric acid affect the synthesis of porous materials, the concentration of hydrochloric acid was reduced (from 0.3 M to 0.02 M and 0.002 M).

2 g of P-123 was dissolved in 6 ml of ethanol. Separately, 3.6 g of precursors were dissolved into 2 ml ethanol and 3 ml of H₂O was added to (samples 13-15) and 0.002 M HCl and the standard procedure was followed.

Study of Effect of Concentration of Surfactant

The amount of P-123, the ratio of surfactant in the total mixture of samples **10-12** was 0.55 before it was decreased to 0.27 in samples **19-21** and increased to 1.1 in samples **22-24**.

4.0 g and 0.5 g of P-123 were dissolved in 6 ml of ethanol respectively and the standard procedure was followed.

Study of Effect of Reaction Time and Aging

Variation in length of hydrothermal treatment/ aging was studied on P-123 samples, the time for refluxing in samples **25-30** decreased from 24 h to 16 h (**25-27**) and 8 h (**28-30**). For samples **31-39**, after refluxing for 24 h they were aged in water bath at 50 °C without stirring for 16 h, 32 h and 48 h samples **31-33**, **34-36**, and **37-39** respectively.

Study of Effect of Precursor

The ratio of TEOS: HPA was also reduced from 0.88:0.12 respectively to 0.75:0.25 and 0.5:0.5 in samples **40-41**, and **42-43** respectively to study how increment in HPA affect materials, then followed the standard procedure.

Chemical Composition

Atomic Absorption Spectroscopy

Calcined samples containing Mo and W were dissolved in hydrofluoric acid, filtered and neutralized with NaOH prior to analysis. The filtrates were collected and analyzed on a Shimadzu AA-6300 atomic absorption spectrophotometer (flame). An external standard method was used to determine absorbance at different concentrations (50 ppm, 100 ppm, 200 ppm, 500 ppm, 1000 ppm) before the calibration curve was determined.

Fourier Transform Infrared Spectroscopy

FT-IR spectra were recorded in KBr pellets on a Vertex 70/80 FT-IR Spectrometer (Bruker Optics, Inc., Billerica, MA).

Structure of Materials

Porosimetry

BET surface area and porosity were measured on a Quantachrome Nova 2200e porosimeter (Boynton Beach, FL). Prior to measurements, the samples were degassed for 2 h at 400 °C in vacuum. The BET surface areas were calculated from the adsorption branch of isotherms in the range $P/P_0 = 0.2-0.5$. Pore size distributions were obtained from desorption branch using BJH method. Micro pore volumes were calculated by DR method. All calculations were performed using NovaWin v.10.01 software.

Particle Size

Particle sizes were determined by dynamic light scattering on a Zetasizer Nano ZS90 (Malvern, UK) with Zetasizer Software v.7.11. The samples were dispersed in water for 10-15mins at sonication prior to analysis.

X-Ray Diffraction

X-ray diffraction (XRD) patterns were recorded on a Dron 2.0 diffractometer (St. Petersburg, Russia) using X-Ray tube with a copper anode and a nickel filter at 30 kV and 15 mA. The patterns were collected in the range of angles 2θ from 5 to 40° that corresponds to a wave vector (q) values 3.6-27.9 nm^{-1} .

Small Angle X-Ray Scattering (SAXS)

Data were obtained using a Kratky camera. Copper anode emission was monochromated by total internal reflection and a nickel filter. Intensity curves were recorded in the step-scanning mode of the scintillation detector. The SAXS curves were recorded in the range of scattering angles from 0.03 – 4.00° ($q=0.022$ - 2.86 nm^{-1}). The curves obtained were smoothed using a FFSAXS program.

Transmission Electron Microscopy (TEM)

Images were obtained on a JEOL 1230 electron microscope (Tokyo, Japan) at 80 kV. Before imaging, samples were dispersed in a 50 % ethanol solution using a W-385 sonicator for 2 min.

CHAPTER 3

RESULTS AND DISCUSSION

Chemical Composition

Samples Synthesized in Standard Conditions

Yields of HPA content of samples synthesized in standard conditions are shown in Table 3.

Table 3: Syntheses of samples in standard conditions

N	Surfactant	HPA	Yield, g/go	Contents of HPA, %
1	DDA	-	0.2	-
2	DDA	Mo	0.27	10.6
3	DDA	W	0.23	1.2
4	SDS	-	0.19	-
5	SDS	Mo	0.21	2.7
6	SDS	W	0.2	0.1
7	TMS	-	0.21	-
8	TMS	Mo	0.19	9.0
9	TMS	W	0.2	6.7
10	P123	-	0.19	-
11	P123	Mo	0.22	7.7
12	P123	W	0.24	7.7

Effects of Varying Conditions

Samples prepared in the presence of P-123 were obtained in different conditions (Table 4) to demonstrate the effects of hydrochloric acid (samples **13-18**), effects of surfactants (samples **19-24**), effects of reaction time (samples **25-30**), effects of aging time (samples **31-39**) and effects of precursors (samples **40-43**).

Table 4: Yields and HPA contents of samples prepared at different conditions

N	HPA	Ratio TEOS:HPA: Pluronic:HCl	Reaction/ aging time, h	Yield, g/g ₀	Contents of HPA, %
1	2	3	4	5	6
13	-	1:0:0.55:0.3:0.002	24/0	0.21	-
14	Mo	0.88:0.12:0.55:0.002	24/0	0.2	3.9
15	W	0.88:0.12:0.55:0.002	24/0	0.22	0.2
16	-	1:0:0.55:0.02	24/0	0.2	-
17	Mo	0.88:0.12:0.55:0.02	24/0	0.23	1.6
18	W	0.88:0.12:0.55:0.02	24/0	0.19	0.9
19	-	1:0:0.27:0.3	24/0	0.26	-
20	Mo	0.88:0.12:0.27:0.3	24/0	0.24	3.5
21	W	0.88:0.12:0.27:0.3	24/0	0.18	4.0
22	-	1:0:1.1:0.3	24/0	0.24	-
23	Mo	0.88:0.12:1.1:0.3	24/0	0.24	2.1
24	W	0.88:0.12:1.1:0.3	24/0	0.15	1.4
25	-	1:0:0.55:0.3	16/0	0.26	-

Table 4 cont'd

1	2	3	4	5	6
26	Mo	0.88:0.12:0.55:0.3	16/0	0.23	8.8
27	W	0.88:0.12:0.55:0.3	16/0	0.24	1.3
28	-	1:0:0.55:0.3	8/0	0.27	-
29	Mo	0.88:0.12:0.55:0.3	8/0	0.22	1.3
30	W	0.88:0.12:0.55:0.3	8/0	0.24	1.8
31	-	1:0:0.55:0.3	24/16	0.21	-
32	Mo	0.88:0.12:0.55:0.3	24/16	0.19	9.6
33	W	0.88:0.12:0.55:0.3	24/16	0.16	0.6
34	-	1:0:0.55:0.3	24/32	0.26	-
35	Mo	0.88:0.12:0.55:0.3	24/32	0.23	3.9
36	W	0.88:0.12:0.55:0.3	24/32	0.24	1.2
37	-	1:0:0.55:0.3	24/48	0.24	-
38	Mo	0.88:0.12:0.55:0.3	24/48	0.2	3.7
39	W	0.88:0.12:0.55:0.3	24/48	0.21	0.6
40	Mo	0.75:0.25:0.55:0.3	24/0	0.19	4.5
41	W	0.75:0.25:0.55:0.3	24/0	0.26	10.4
42	Mo	0.5:0.5:0.55:0.3	24/0	0.13	6.0
43	W	0.5:0.5:0.55:0.3	24/0	0.14	9.5

Fourier Transform Infrared Spectroscopy (FT-IR)

FT-IR spectra of all samples (Fig.12) have specific absorption bands of silica gel. Unmodified product has bands at the following wavenumbers (cm^{-1}): 459 ($\delta\text{Si-O-Si}$), 818 ($\nu_{\text{s}}\text{Si-O-Si}$), 1081 ($\nu_{\text{as}}\text{Si-O-Si}$), 1640 (adsorbed H_2O) and 3457 (νOH). The first band was shifted in PMA-modified samples to 461 cm^{-1} that is the result of overlapping with bands $\delta\text{Mo-O-Mo}$ (464 cm^{-1}). For PTA-modified samples it was shifted to 454 cm^{-1} . The second band was shifted to 805 cm^{-1} . The band of silanol groups shifted in the case of PTA-containing sample only. In addition, new strong band at 862 cm^{-1} appeared in the spectra of modified silica gels. This band is typical for Keggin's structure of heteropolyacids and corresponds to $\nu_{\text{as}}\text{Mo-O-Mo}$ or $\nu_{\text{as}}\text{W-O-W}$ vibrations.

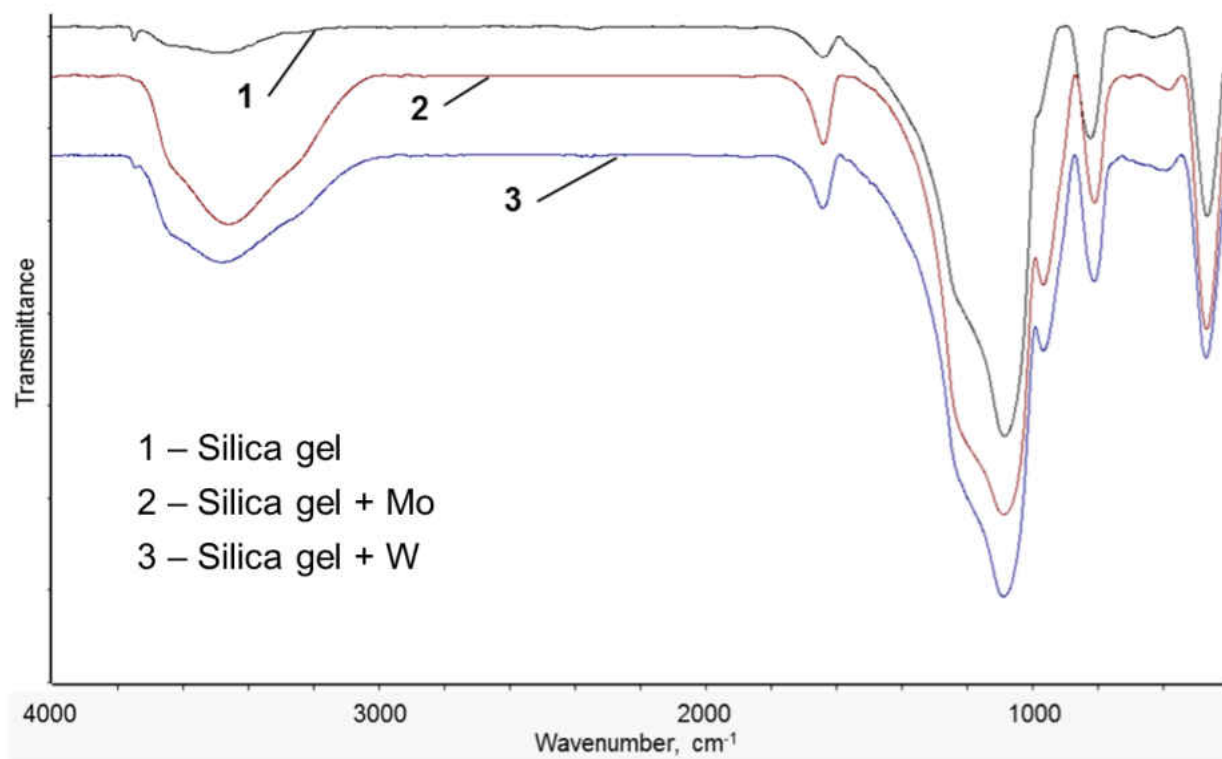


Figure 12: FT-IR spectra of the materials

Structural Characteristics

Porosity of Samples

Adsorption isotherms of all samples displayed their mesoporous structure. As is evident (Fig. 13), all isotherms belong to the type IV with different types of hysteresis loops. The isotherms of samples obtained with DDA and P123 had shapes of the H1 type typical for cylindrical pores. Use of TMS resulted in products with narrow slit pores including micropores (type H4). In the case of SDS, the shape of hysteresis loop of H4 type was characteristic for plate-like particles. The data on BET surface areas and pore sizes are presented in Table 5. All samples have both mesopores and micropores. Aging of the reaction mixture significantly reduced not only BET surface areas but also pore volumes.

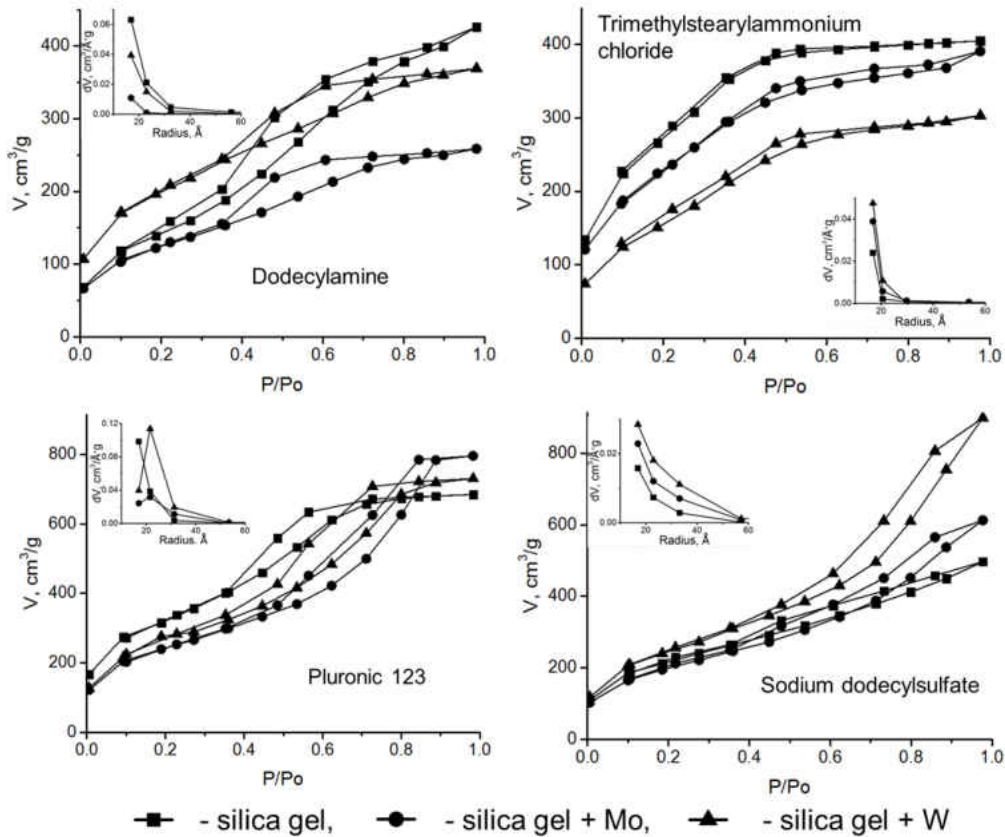


Figure 13: Nitrogen adsorption isotherms on materials obtained with different templates

Table 5: Porosity of samples

N	BET surface area, m ² /g	Pore volume, cm ³ /g	Micropore volume,cm ³ /g	Average pore radius, Å
1	2	3	4	5
1	542	0.59	0.42	16.9
2	424	0.10	0.31	22.7
3	676	0.35	0.46	16.9
4	538	0.36	0.52	22.8
5	677	0.65	0.53	22.6
6	870	1.24	0.68	16.9
7	1006	0.15	0.57	16.9
8	836	0.26	0.51	16.7
9	635	0.35	0.39	21.6
10	1123	0.82	0.82	16.9
11	812	0.97	0.67	33.3
12	900	1.02	0.72	21.6
13	838	0.19	0.52	16.9
14	592	0.02	0.37	22.7
15	639	0.08	0.40	16.7
16	754	0.20	0.48	16.8
17	461	0.05	0.29	22.5
18	759	0.22	0.49	16.9
19	682	0.11	0.43	16.9
20	656	0.34	0.45	16.9

Table 5 cont'd

1	2	3	4	5
21	574	0.03	0.37	22.3
22	875	0.47	0.60	17.0
23	790	0.40	0.54	16.9
24	748	0.19	0.47	16.7
25	827	0.27	0.51	16.9
26	705	0.32	0.45	16.9
27	665	0.20	0.42	16.7
28	801	0.23	0.54	16.8
29	709	0.21	0.47	16.7
30	669	0.15	0.42	16.9
31	860	0.33	0.57	16.9
32	733	0.42	0.51	16.9
33	784	0.29	0.52	16.9
34	820	0.31	0.54	16.9
35	685	0.22	0.45	17.0
36	735	0.14	0.51	22.9
37	719	0.38	0.50	16.9
38	681	0.23	0.44	16.9
39	782	0.28	0.51	16.6
40	659	0.51	0.51	17.0
41	514	0.30	0.38	16.9
42	709	0.57	0.57	17.0

Table 5 cont'd

1	2	3	4	5
43	397	0.05	0.29	22.6

Particle Size and Polydispersity Index (PDI)

Most of the samples had particle size in the range of 500-1100 nm (Table 6). Particle size distribution data showed presence of a major fraction of 1-2 μm and a minor fraction of smaller particles of 100-200 nm in diameter. The only exception was sample 9, which had a significantly lower particle size of 59 nm.

X-Ray Diffraction (XRD) and Small Angle X-Ray Scattering (SAXS)

X-ray diffraction patterns of all samples (Figure 14a) display very broad bands, which are characteristic for amorphous materials. The diffraction maxima ($2\theta^\circ$) were almost similar for diffractograms 1 (22.6) and 2 (22.7), which correspond to periodicity length (average size of repeating units) 0.393-0.392 nm. In the diffractogram of 3, it was shifted to 22.3 that indicates increasing of periodicity length to 0.399 nm. No patterns of isolated heteropolyacids were observed.

SAXS curves of the samples (Figure 14b) have primary linear region with slope values of -3.2 to -3.3. The curves 1 and 2 have clear maxima at $q=0.050$ and 0.045 \AA^{-1} , respectively.

Calculation of pore sizes using Bragg's law gives 12.5 nm for non-modified silica gel and 13.6 nm for PMA-containing sample. The next linear region shows mass fractals of highly branched structure for these materials. The curve 3 does not display a maximum that is an evidence of high polydispersity of pores in PTA-containing sample. In this case pore sizes were calculated using Guinier approach and found 16 nm. This material had low branched structure.

Table 6: Particle size and PDI

N	Average particle size, nm	PDI	N	Average particle size, nm	PDI
1	844	0.53	23	762	0.24
2	351	0.47	24	582	0.11
3	868	0.42	25	1046	0.32
4	1139	0.34	26	693	0.28
5	1082	0.1	27	1035	0.12
6	875	0.3	28	1013	0.26
7	934	0.26	29	816	0.23
8	837	0.28	30	986	0.43
9	59	0.24	31	668	0.48
10	1046	0.32	32	893	0.46
11	933	0.2	33	927	0.28
12	740	0.33	34	1178	0.21
13	711	0.44	35	955	0.27
14	946	0.37	36	902	0.28
15	747	0.49	37	1206	0.18
16	591	0.48	38	975	0.39
17	955	0.32	39	939	0.4
18	644	0.51	40	745	0.39
19	971	0.2	41	745	0.29
20	891	0.38	42	640	0.48
21	801	0.48	43	406	0.48
22	955	0.29			

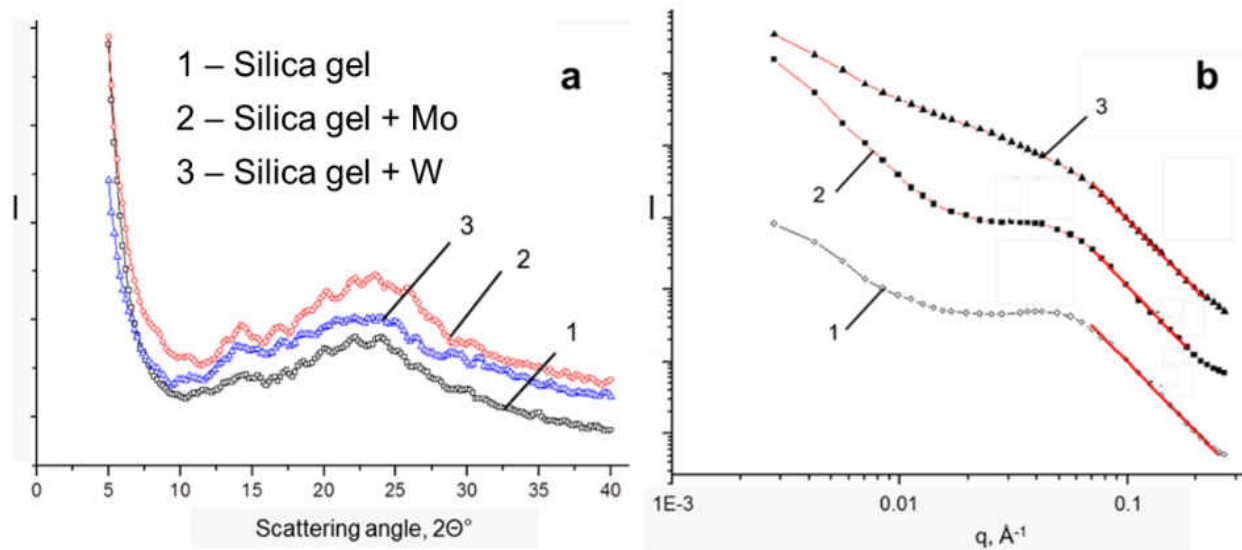


Figure 14: XRD (a) and SAXS (b) curves of the materials, obtained with P-123

Tem Imaging

All samples were porous with pore size 1-3 nm (Figure 15). It is evident that porous system is not ordered with non-uniform size distributions. The sizes of agglomerates were 1-5 μm , however, smaller particles 100-500 nm were also found.

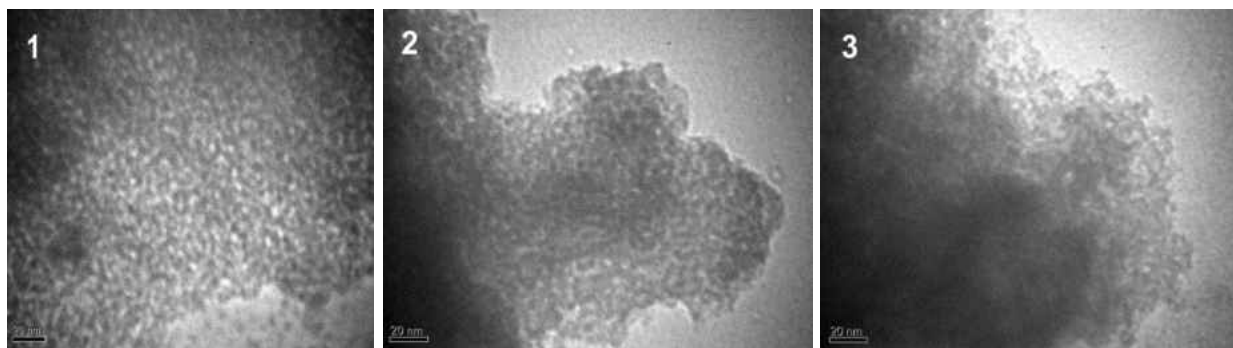


Figure 15. TEM images of non-modified (1), Mo-containing (2), and W-containing silica gel (3)

Discussion

The reaction of co-condensation of TEOS with HPAs is very sensitive to the synthetic protocol. In most of syntheses, the yields of the products obtained with or without HPAs were almost similar. Presence of characteristic band of Keggin's structure at 862 cm^{-1} in FT-IR spectra along with absence of XRD patterns of HPAs at $2\Theta = 23^\circ$ (PTA) and 27° (PMA) proved fine dispersing of HPAs in the silica network. Incorporation of large PTA molecules into silica network reduced d-spacing from 0.69 to 0.56 Å. Presence of PMA did not affect this parameter. It should be noted that partial leaching of PMA occurred from the sample that was evident from characteristic color of 'heteropoly blue' of the solution. In the case of PTA, no leaching was detected.

All materials were mesoporous with the presence of micropores. However, their structural characteristics depended on the conditions of the synthesis. The effect of template nature on porosity was determined using surfactants that belong to all types: cationic (DDA and TMS), anionic (SDS), and non-ionic (P-123). All syntheses were carried out in acidic media, thus the types of silanol-surfactant interactions were $\text{S}^+\text{X}^-\text{I}^+$, S^-I^+ , and $(\text{S}^0\text{H}^+)\text{X}^-\text{I}^+$, respectively. The pore size is controlled by various factors, including degree of surfactant ionization. In addition, HPAs may contribute to the silica network stabilization by playing the role of counterions to protonated silanol groups $(\equiv\text{Si}-\text{OH}_2)^+(\text{H}_2\text{PW}_{12}\text{O}_{40})^-$. The widest pore size distribution was found in the samples **4-6** obtained with SDS. We associate this characteristic with partial protonation of sulfate group that weakened their interaction with $\equiv\text{Si}-\text{OH}_2^+$.

The highest BET surface area was achieved at the use of P-123 (samples **10-12**). These samples also have the highest pore volumes. Large molecules of this surfactant can self-assemble

with the silica species and form larger pores [1]. This effect was especially clear in the samples **11** and **12** with PMA and PTA.

It is interesting that, at the use of cationic surfactants, pore volume of HPA-containing products decreased. In the case of anionic or non-ionic surfactant, the effect of HPAs was reversed. This effect can be attributed to the side reaction between HPAs and ammonium ion leading to partial precipitation of the salt in pores.

Unusually low size of particles of sample **9** (Fig. 16) can be explained by stabilization of primarily formed silica nanoparticles. TMS reacted with surface PTA in the silica network and formed protective shell preventing agglomeration. Ionic bond $[\text{C}_{18}\text{H}_{37}(\text{CH}_3)_3\text{N}]^+[\text{H}_2\text{PW}_{12}\text{O}_{40}]^-$ is stable even in acidic media.

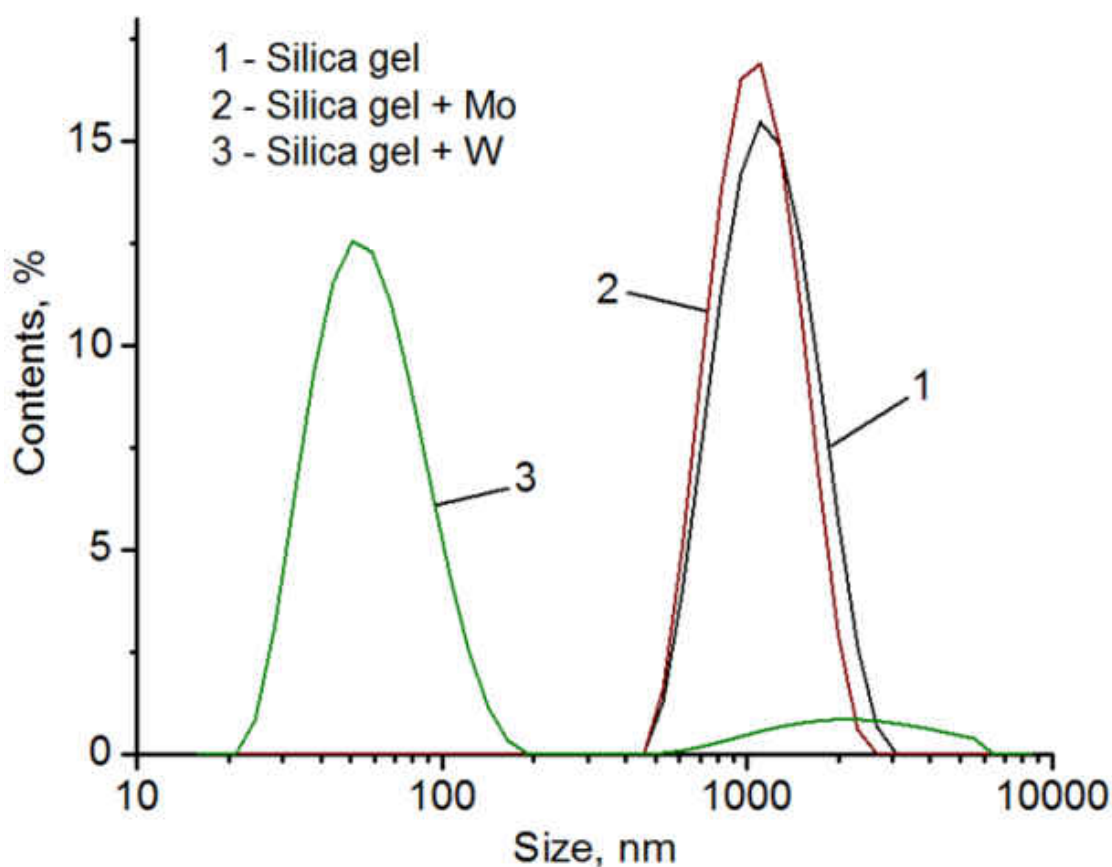


Figure 16: Particle size distribution in samples obtained with TMS

Study of the effect of reaction time on yields and characteristics of silica gels (samples **25-30**) showed that the yields of solid products were independent on duration of the synthesis while porosity increased with time. It is well known that polycondensation of TEOS in acidic media occurs through preferable hydrolysis of less sterically hindered terminal $\equiv\text{Si-OEt}$ groups. This process results in linear low-branched structures of a polymer. These structures have lower BET surface areas and pore volumes. At longer time, degree of cross-linking increases leading to formation of new pores and increased surface areas of the silica gels.

Similar effect was observed at aging of the reaction mixtures (samples **31-39**). Pore volumes in the samples obtained with aging reduced in comparison with non-aged samples. Their BET surface areas were lower too. It should be noted that any variations in the synthesis duration did not affect micropore volumes. Micropores probably were formed due to entrapment of surfactant molecules in the silica walls prior to calcination independently on the reaction conditions. Aging increased average particle sizes of the products [39].

Formation of gel in acidic media proceeds in accordance with cluster-cluster growth model. Reduced concentration of acid (samples **13-18**) resulted in slower polycondensation and less developed porous system. Especially it was evident from the pore volumes of samples **14** and **15**. Concentration of surfactant is also one of essential parameters of the synthesis (samples **19-24**). Porosity of silica gel notably drops in the case of insufficient amount of template. However, higher concentration of surfactant also reduces BET surface area and pore volume that might be caused by shrinkage of pores at calcination. It was found earlier that high surfactant concentration favors shrinkage. As it was expected, particle size increased at higher concentration of P-123 [42].

Increased amount of PMA in the reaction mixture did not change characteristics of the products while high contents of PTA dramatically reduced porosity. It was evident that high contents of PTA leads to aggregation and pore blocking.

Conclusions

- Mesoporous materials containing PMA and PTA were synthesized in various conditions.
- No leaching of PTA was observed from the silica gel.
- Cationic surfactants might react with HPAs in the silica pores reducing their volumes.

However, TMS provided a stabilizing effect on primary nanoparticles containing PTA and prevented agglomeration.

- Aging increased average particle size but reduced porosity.
- The ratio of PTA: TEOS in the reaction mixture should not exceed 0.25:0.75 to prevent pore blocking.
- The obtained results enabled development of an adsorbent with high surface area and high contents of accessible HPA adsorption sites. This adsorbent may be used for immobilization of contaminants that hardly form insoluble compounds, i.e. radioactive caesium.

References

1. Zhao, D. Y.; Feng, J. L.; Huo, Q. S.; Melosh, N.; Fredrickson, G. H.; Chmelka, B. F.; Stucky G. D. Triblock copolymer syntheses of mesoporous silica with periodic 50 to 300 angstrom pores. *Science* **1998**, 279, 548.
2. Clark, H.; Macquarrie, D. J.; Tavener, S. J. The application of modified mesoporous silicas in liquid phase catalysis. *Dalton Trans.* **2006**, 4297.
3. Wan, Y.; Shi, Y.; Zhao, D. Supramolecular aggregates as templates: ordered mesoporous polymers and carbons. *Chem. Mater.* **2008**, 20, 932.
4. Taguchi, A.; Schuth F. Ordered mesoporous materials in catalysis. *Micropor. Mesopor. Mat.* **2005**, 77, 1.
5. Yang, Q.; Liu, J.; Yang, J.; Zhang, L.; Feng, Z.; Zhang, J.; Li, C. Acid catalyzed synthesis of ordered bifunctionalized mesoporous organosilicas with large pore. *Micropor. Mesopor. Mat.* **2005**, 77, 257.
6. Yang, Q.; Liu, J.; Yang, J.; Kapoor, M. P.; Inagaki, S.; Li, C. Synthesis, characterization, and catalytic activity of sulfonic acid-functionalized periodic mesoporous organosilicas. *J. Catal.* **2004**, 228, 265.
7. Li, K.; Hu, J.; Li, W.; Ma, F.; Xu, L.; Guo, Y. Design of mesostructured H₃PW₁₂O₄₀-silica materials with controllable ordered and disordered pore geometries and their application for the synthesis of diphenolic acid. *J. Mater. Chem.* **2009**, 19, 8628.
8. Yu, J.; Shi, J. L.; Chen, H. R.; Yan, J. N.; Yan, D. S. Effect of inorganic salt addition during synthesis on pore structure and hydrothermal stability of mesoporous silica. *Micropor. Mesopor. Mat.* **2001**, 46, 153.

9. Katiyar, A.; Yadav, S.; Smirniotis, P. G.; Pinto, N. G. Synthesis of ordered large pore SBA-15 spherical particles for adsorption of biomolecules. *J. Chromatogr. A* **2006**, 1122, 13.
10. Kresge, C. T.; Roth, W. J. The discovery of mesoporous molecular sieves from the twenty year perspective. *Chem. Soc. Rev.* **2013**, 42, 3663.
11. Nandiyanto, A. B. D.; Kim, S. G.; Iskandar, F.; Okuyama, K.; Synthesis of silica nanoparticles with nanometer-size controllable mesopores and outer diameters. *Micropor. Mesopor. Mat.* **2009**, 120, 447.
12. Xiao, C.; Fujita, N.; Miyasaka, K.; Sakamoto, Y.; Terasaki, O.; Dodecagonal tiling in mesoporous silica. *Nature* **2012**, 487, 349.
13. Ojo, O. K.; Golovko, L. V.; Gomza, Y. P.; Vasiliev, A. N. Mesoporous silsesquioxanes with high contents of surface amine groups. *Silicon* **2012**, 4, 189.
14. Mastuli, M. S.; Ansari, N. S.; Nawawia, M. A.; Mahat, A. M. Effects of cationic surfactant in sol-gel synthesis of nano-sized magnesium oxide. *APCBEE Procedia.* **2012**, 3, 93.
15. Berthod, A. Mise au point structures physico-chimiques des milieux disperses, micelles, emulsions et microémulsions. *J. Chim. Phys.* **1983**, 80, 407.
16. Corma, A. From microporous to mesoporous molecular sieve materials and their use in catalysis. *Chem. Rev.* **1997**, 97, 2373.
17. Newman, A. D.; Lee, A. F.; Wilson, K.; Young, N. A. On the active site in $\text{H}_3\text{PW}_{12}\text{O}_{40}/\text{SiO}_2$ catalysts for fine chemical synthesis. *Catal. Lett.* **2005**, 102, 45.
18. Okuhara, T. Water-tolerant solid acid catalysts. *Chem. Rev.* **2002**, 102, 3641.
19. Okuhara, T.; Watanabe, H.; Nishimura, T.; Inumaru, K.; Misono, M. Microstructure of cesium hydrogen salts of 12-tungstophosphoric acid relevant to novel acid catalysis. *Chem. Mater.* **2000**, 12, 2230.

20. Drago, R. S.; Dias, J. A.; Maier, T. O. An acidity scale for Brønsted acids including $\text{H}_3\text{PW}_{12}\text{O}_{40}$. *J. Am. Chem. Soc.* **1997**, 119, 7702.
21. Kozhevnikov, I. V. Advances in catalysis by Heteropolyacids. *Russ. Chem. Rev.* **1987**, 56, 811.
22. Yang, L.; Qi, Y.; Yuan, X.; Shen, J.; Kim, J. Direct synthesis, characterization and catalytic application of SBA-15 containing heteropolyacid $\text{H}_3\text{PW}_{12}\text{O}_{40}$. *J. Mol. Catal. A: Chem.* **2005**, 229, 199.
23. Okuhara, T.; Nishimura, T.; Misono, M. Novel microporous solid “superacids” $\text{Cs}_x\text{H}_{3-x}\text{PW}_{12}\text{O}_{40}$ ($2 \leq x \leq 3$), Proceedings of the 11th ICC, Baltimore, MD, USA, June 30-July 5, 1996 (*Studies in surface science and catalysis*, v. 101); Hightower, J. W.; Delgass, W. N.; Iglesia, E.; Bell A.T. Eds.; Elsevier: Amsterdam, 1996; 581.
24. Kozhevnikov, I. V. Heteropolyacids and related compounds as catalysts for fine chemical synthesis. *Cat. Rev. - Sci. Eng.* **1995**, 37.
25. Rao, P. M.; Landau M. V.; Wolfson, A.; Shapira-Tchelet, A. M.; Herskowitz, M. Cesium salt of a heteropolyacid in nanotubular channels and on the external surface of SBA-15 crystals: preparation and performance as acidic catalysts. *Micropor. Mesopor. Mat.* **2005**, 80, 43.
26. Popa, A.; Sasca, V.; Verdes, O.; Barvinschi, P.; Holclajtner-Antunović, I. Acidic and neutral cesium salts of 12-molybdophosphoric acid supported on SBA-15 mesoporous silica. The influence of Cs concentration and surface coverage on textural and structural properties. *Mater. Res. Bull.* **2014**, 50, 312.
27. Silva, A. R.; Wilson, K.; Whitwood, A. C.; Clark, J. H.; Freire, C. E. Amine-functionalised hexagonal mesoporous silica as support for copper (II) acetylacetonate catalyst. *J. Inorg. Chem.* **2006**, 6, 1275.

28. Ras, E. J.; Rothenberg, G. Heterogeneous catalyst discovery using 21st century tools: a tutorial. *RSC Adv.* **2014**, 4, 5963.
29. Haber, J.; Block, J. H.; Delmon, B. Manual of methods and procedures for catalyst characterization. *Pure Appl. Chem.* **1995**, 67, 1257.
30. Ji, X.; Lee, K. T.; Holden, R.; Zhang, L.; Zhang, J.; Botton, G. A.; Couillard, M.; Nazar, L. F. Nanocrystalline intermetallics on mesoporous carbon for direct formic acid fuel cell anodes. *Nat. Chem.* **2010**, 2, 286.
31. Yokoi, T.; Yoshitake, H.; Yamada, T.; Kubota, Y.; Tatsumi, T. Amino-functionalized mesoporous silica synthesized by a novel synthesis route using an anionic surfactant. *J. Mater. Chem.* **2006**, 16, 1125.
32. Li, K.; Hu, J.; Li, W.; Ma, F.; Xu, L.; Guo, Y. Design of mesostructured $\text{H}_3\text{PW}_{12}\text{O}_{40}$ -silica materials with controllable ordered and disordered pore geometries and their application for the synthesis of diphenolic acid. *J. Mater. Chem.* **2009**, 19, 8628.
33. Guo, Y.; Li, K.; Yu, X.; Clark, J. H. Mesoporous $\text{H}_3\text{PW}_{12}\text{O}_{40}$ -silica composite: Efficient and reusable solid acid catalyst for the synthesis of diphenolic acid from levulinic acid. *Appl. Catal. B: Environ.* **2008**, 81, 182.
34. Dong, B. B.; Zhang, B. B.; Wu, H. Y.; Li, S. D.; Zhang, K.; Zheng, X. C. Direct synthesis, characterization and application in benzaldehyde oxidation of HPWA-SBA-15 mesoporous catalysts. *Micropor. Mesopor. Mat.* **2013**, 176, 186.
35. Sheng, X.; Kong, J.; Zhou, Y.; Zhang, Y.; Zhang, Z.; Zhou, S. Direct synthesis, characterization and catalytic application of SBA-15 mesoporous silica with heteropolyacid incorporated into their framework. *Micropor. Mesopor. Mat.* **2014**, 187, 7.

36. Hoo, P. Y.; Abdullah, A. Z. Direct synthesis of mesoporous 12-tungstophosphoric acid SBA-15 catalyst for selective esterification of glycerol and lauric acid to monolaurate. *Chem. Eng. J.* **2014**, 250, 274.
37. Kaleta, W.; Nowinska, K. Immobilisation of heteropoly anions in Si-MCM-41 channels by means of chemical bonding to aminosilane groups. *Chem. Commun.* **2001**, 535.
38. Kala Raj, N. K.; Deshpande, S. S.; Ingle, R. H.; Raja, T.; Manikandan, P. Heterogenized molybdovanadophosphoric acid on amine-functionalized SBA-15 for selective oxidation of alkenes. *Catal. Lett.* **2004**, 98, 217.
39. Izumi, Y.; Hisano, K.; Hida, T. Patent report. *Appl. Catal. A.* **1999**, 181, 277.
40. Nowin'ska, K.; Fórmaniak, R.; Kaleta, W.; Waław, A. Heteropoly compounds incorporated into mesoporous material structure. *Appl. Catal. A.* **2003**, 256, 115.
41. Zhu, M.; Gao, X.; Luo, G.; Dai, B. A novel method for synthesis of phosphomolybdic acid-modified Pd/C catalysts for oxygen reduction reaction. *J. Power Sources.* **2013**, 225, 27.
42. Feng, P.; Bu, X.; Pine, D. J. Control of pore sizes in mesoporous silica templated by liquid crystals in block copolymer-cosurfactant-water systems. *Langmuir.* **2000**, 16, 5304.

VITA

ADETOLA OPEYEMI

- Education:** B.Sc. Industrial Chemistry, University of Ilorin, Nigeria. 2012
MS Chemistry, East Tennessee State University, Johnson City, TN. 2016
- Employment:** Analytical Chemist, American Toxicology Lab. Johnson City, TN. (March, 2016- present)
- Professional Experience:** Graduate Assistant, East Tennessee State University, Chemistry Department, College of Arts and sciences, Johnson City, TN. (2015-2016)
Chemistry Teacher, Shiloh Hill College, Edo state, Nigeria, (2012-2013)
- Presentations:** Adetola Opeyemi, Leonid Golovko and Aleksey Vasiliev “Modification of Silica Gel by Heteropolyacids” 6th International Conference on Advanced Materials Research (ICAMR) Torino, Italy, Jan 22-24, 2016, Paper ID: E017

Aleskey Vasiliev, Adetola Opeyemi “Superacidic Mesoporous Materials” 250th ACS National Meeting in Boston, Massachusetts, August 16-20, 2015 Abstr: 501

Adetola Opeyemi, Leonid Golovko and Aleksey Vasiliev “Mesoporous Materials containing Heteropolyacids” 67th Southeast Regional Meeting of the American Chemical Society, Memphis, TN, November 4-6, 2015, Abstr: SERMACS-86.
- Publication:** Adetola, Opeyemi; Golovko, Leonid; Vasiliev, Aleksey, Modification of Silica Gel by Heteropolyacids, Key Engineering Materials, **2016**, 689,126.
- Grant:** Adetola Opeyemi, Aleskey Vasiliev, ETSU School of Graduate Studies and ETSU Graduate Council Research Grants (2014-2015) “Superacidic mesoporous materials“, funded: \$785
- Activity:** Committee Member, East Tennessee State University Graduate and Professional Students Association (2015-2016)